

# A Career in Catalysis: John E. Bercaw

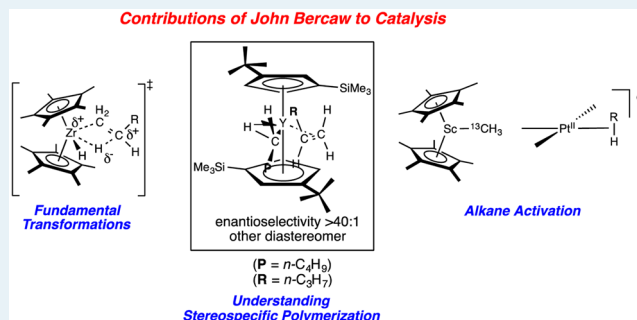
Peter T. Wolczanski<sup>\*,†</sup> and Paul J. Chirik<sup>\*,‡</sup>

<sup>†</sup>Department of Chemistry and Chemical Biology, Baker Laboratory, Cornell University, Ithaca, New York 14853, United States

<sup>‡</sup>Department of Chemistry, Princeton University, Princeton, New Jersey 08544, United States

**ABSTRACT:** On the occasion of Professor John Bercaw's 70th birthday, we reflect and highlight his distinguished career in organometallic chemistry and homogeneous catalysis. What began as a fundamental interest in the chemistry of bis(cyclopentadienyl)titanium compounds and their interaction with molecular nitrogen evolved into a vibrant and diverse program tackling some of the most important problems in catalysis. Using well-defined organometallic compounds, fundamental insights were gained in the mechanism of CO reduction; basic transformations of organometallic chemistry, such as alkene insertion and alkyl  $\beta$ -hydrogen elimination; the origin of stereocontrol in metallocene-catalyzed polymerization; and in the activation of hydrocarbons by electrophilic late transition metals.

**KEYWORDS:** CO reduction, metallocene, polymerization, C–H activation



## 1. INTRODUCTION

On August 10–12, 2014 at the 248th National Meeting of the American Chemical Society in San Francisco, CA, former and current students and postdocs, friends, and colleagues from around the globe gathered for a symposium on the occasion of John Bercaw's 70th birthday (Figure 1). It was a fitting tribute to an outstanding scientist, who not only helped to define the field of organometallic chemistry but also educated and trained

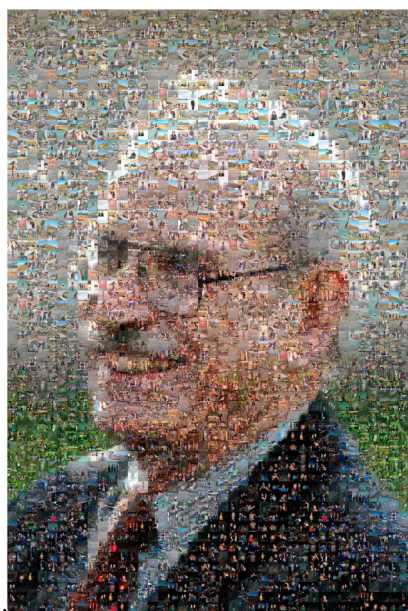


**Figure 1.** A mural of John Bercaw comprised of individual photographs of his co-workers, friends, and colleagues.

generations of new scientists that contribute in academia, industry, and national laboratories. It was this latter contribution that was most brilliantly on display in San Francisco as the presentations illustrated how John's influence and approach to science extends beyond organometallic chemistry and is now impacting fields as disparate as organic synthesis, nanoscience, alternative energy, and materials chemistry.

Beginning with his Ph.D. studies at the University of Michigan with Hans Brintzinger, John has always been interested in answering fundamental questions that ultimately have broad impact. From elucidation of the structure of "titanocene" to understanding the reduction of carbon monoxide relevant to the Fischer–Tropsch process, to alkene polymerization and alkane functionalization, John Bercaw has tackled some of the most significant and challenging problems in catalysis. The Bercaw approach is characterized by the intersection of innovative organometallic synthesis coupled with clever experiments designed to unravel the most complicated mechanistic puzzles. First and foremost, however, John Bercaw is an educator. From the classroom to discussing the latest results over coffee, John's primary focus has been the welfare and education of his co-workers and colleagues. John is famous for saying you do not work "for him" but rather "with him". The mural presented in Figure 1 is emblematic of this collegial spirit as co-workers, friends, and colleagues provided individual photographs to define an outstanding scientist. In this Account, we highlight some of John's many contribution to catalysis. Perhaps more significant than the conclusions is how

**Received:** January 15, 2015

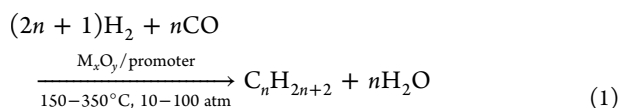
**Revised:** February 4, 2015

**Published:** February 9, 2015

the story was uncovered: it is this signature Bercaw approach to chemistry that will surely be one of the most significant aspects of John Bercaw's legacy.

## 2. CARBON MONOXIDE REDUCTION

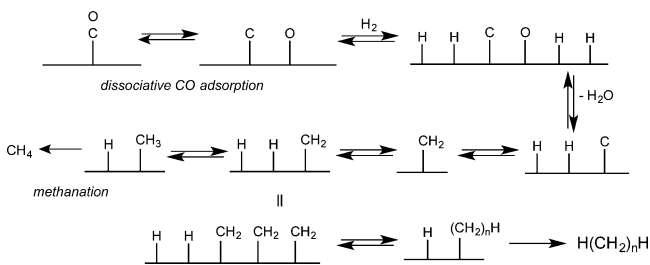
The OPEC oil embargo of 1973 and concerns regarding future production in the United States prompted a renewed interest in Fischer–Tropsch (F–T)<sup>1</sup> chemistry when Bercaw initiated his independent career. A perusal of the literature of this period, especially in catalysis and related engineering disciplines, begged for greater mechanistic understanding of the F–T process, the conversion of syngas, carbon monoxide, and dihydrogen, to hydrocarbons. Shown in eq 1 is a simple description of the F–T reaction as applied to the synthesis of hydrocarbons.



The actual complexity of the process, in terms of the myriad catalysts/promoters and product variation (e.g., oxygenates) cannot be overstated, but the critical reactions can be narrowed to microscopic events featuring C–O bond-breaking and C–C and C–H making. It is these steps that the purveyors of organometallic chemistry sought to model, with potential homogeneous catalysis in mind.

Shown in Scheme 1 is a typical “carbon on a stick” mechanistic scheme from the early 1970s that provides the

**Scheme 1. Model of the Surface-Catalyzed Fischer–Tropsch Reaction**



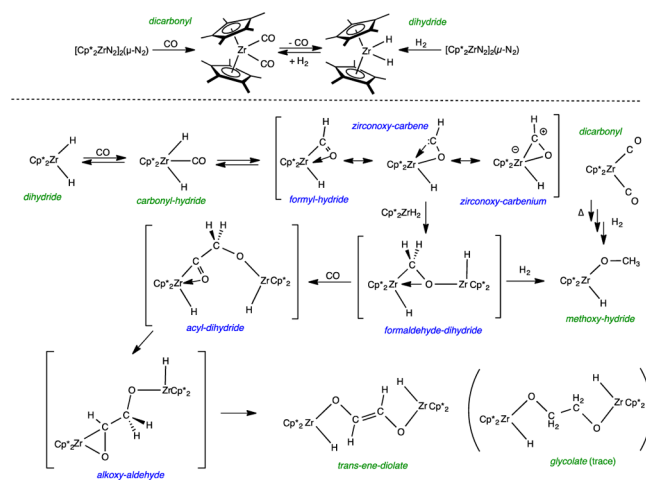
essence of the F–T process, yet is bereft of a realistic portrayal, especially in valence bond or molecular language, of the actual surface species or their plausible generation, as in the case of surface hydrocarbyls. Although the dissociative adsorption of carbon monoxide had been identified as a plausible first step and its hydrogenation and subsequent polymerization of –CH<sub>2</sub>– was logical, it was unknown whether the actual F–T process incorporated –CHO, CH<sub>2</sub>OH, –COCH<sub>3</sub> or like species in the actual deoxygenation step(s). Such surface fragments appeared to be crucial intermediates in the F–T process that produced oxygenates, which also proved to be important targets for homogeneous catalysis involving syngas.

In modeling steps of the F–T reaction, the harsh conditions employed in heterogeneous catalysis were a cause for concern. Typical late metal carbonyls would add dihydrogen, but C–O bond-breaking and C–H bond-making reactions were initially not observed, and metal carbide formation proved dominant in clusters. A means of compensating for higher temperatures and pressures proved to be the use of early transition metals, whose

oxophilicity was exploited to drive the reduction of carbon monoxide, and John Bercaw provided the pioneering effort.<sup>2</sup>

Scheme 2 portrays some of the initial findings of the Bercaw group, which included one of the first C–C couplings

**Scheme 2. Reduction of CO by Zirconocene Complexes**

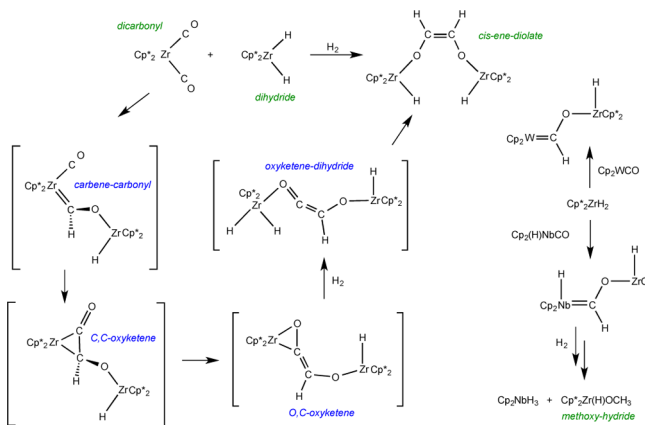


generated solely from CO.<sup>3</sup> The key molecules in the chemistry were the dicarbonyl, Cp\*<sub>2</sub>Zr(CO)<sub>2</sub>, and the dihydride, Cp\*<sub>2</sub>ZrH<sub>2</sub> (Cp\* = η<sup>5</sup>-C<sub>5</sub>Me<sub>5</sub>), which were simply prepared via the addition of CO and H<sub>2</sub> to the dinitrogen complex, [Cp\*<sub>2</sub>(N<sub>2</sub>)Zr]<sub>2</sub>(μ-N<sub>2</sub>), respectively. Thermolysis of the dicarbonyl in the presence of dihydrogen led to the methoxyhydride, Cp\*<sub>2</sub>Zr(H)OCH<sub>3</sub>, but the low temperature carbonylation of the dihydride afforded the *trans*-ene-diolate, [Cp\*<sub>2</sub>(H)Zr]<sub>2</sub>(μ-*trans*-OCH=CHO). Methoxyhydride formation was later realized as occurring via conversion of the dicarbonyl to the dihydride and subsequent carbonylation in the presence of excess H<sub>2</sub>; hence, the two products shared a likely common intermediate, the formaldehyde dihydride, Cp\*<sub>2</sub>(H)ZrCH<sub>2</sub>OZr(H)Cp\*<sub>2</sub>. Low-temperature IR evidence for the initial carbonylation product, the carbonyl dihydride, was obtained in collaboration with Ken Caulton,<sup>4</sup> and Bercaw's prediction that the electron density in the Zr–H bonds would contribute in “backbonding” to the carbonyl was borne out by its 2044 cm<sup>−1</sup> stretching frequency. The subsequent formation of a formylhydride was a logical step toward further reduction of the initial CO by a second equivalent of dihydride, and the ensuing chemistry evoked an “oxycarbene” structure to reconcile C=C bond formation. Calculations by Hoffmann<sup>5</sup> and Hofmann<sup>6</sup> and co-workers focused in on a carbenium structure as being most likely, as examples of hydride transfer to related species were discovered.<sup>7</sup> Once formation of the formaldehyde dihydride occurred, partitioning to the two products depended on the conditions, and with excess CO, a second insertion afforded the acyl dihydride, Cp\*<sub>2</sub>(H)Zr(μ-COCH<sub>2</sub>O)Zr(H)Cp\*<sub>2</sub>. Carbon–hydrogen bond formation to generate the alkoxyaldehyde, Cp\*<sub>2</sub>Zr(μ-OCHCH<sub>2</sub>O)Zr(H)Cp\*<sub>2</sub>, provided a path to the final *trans*-ene-diolate via β-H-elimination.<sup>8</sup> Its intermediacy also provided a rationale for the *trans* geometry of the product, as the steric interactions of the two Cp\*<sub>2</sub>Zr fragments are minimized in the appropriate conformation.

Additional CO reduction chemistry was examined in the context of binuclear hydride transfer to bound CO, as the combination of Cp\*<sub>2</sub>Zr(CO)<sub>2</sub> and Cp\*<sub>2</sub>ZrH<sub>2</sub> in the presence of

dihydrogen afforded yet another product, the *cis*-ene-diolate,  $[\text{Cp}^*_2(\text{H})\text{Zr}]_2(\mu\text{-cis-OCH=CHO})$ , shown in Scheme 3. Here,

### Scheme 3. Mechanism of CO Reduction



the reduction of a bound carbonyl by the dihydrogen was proposed to afford the carbene carbonyl,  $\text{Cp}^*_2(\text{CO})\text{Zr}=\text{CHOZr}(\text{H})\text{Cp}^*_2$ . A subsequent coupling of carbonyl and zirconoxycarbene fragments can yield the C,C-oxyketene-C,C,  $[\text{Cp}^*_2\text{Zr}](\mu\text{-C,C-OCCHO})[\text{Zr}(\text{H})\text{Cp}^*_2]$ , which is prone to rearrange to its O,C-oxyketene isomer due to steric influences and the oxophilicity of zirconium. Dihydrogen addition and ketene reduction from its most sterically favorable side provides the logic for the observed *cis* stereochemistry of the product.<sup>2,9,10</sup>

The idea that a transition metal hydride could reduce a bound carbonyl in homogeneous solution had little precedent; hence,  $\text{Cp}_2\text{WCO}$  and  $\text{Cp}_2\text{Nb}(\text{CO})\text{H}$  were selected for independent trials. As Scheme 3 also shows, those substrates yielded the zirconoxycarbenes  $\text{Cp}_2\text{W}=\text{C}(\text{H})\text{OZr}(\text{H})\text{Cp}^*$  and  $\text{Cp}_2(\text{H})\text{Nb}=\text{C}(\text{H})\text{OZr}(\text{H})\text{Cp}^*_2$ , respectively.<sup>11</sup> As a bonus, the niobium zirconoxycarbene was later revealed to undergo insertion reactions, such as that shown in the presence of  $\text{H}_2$ . The methoxyhydride  $\text{Cp}^*_2(\text{H})\text{ZrOCH}_3$  was generated in a step germane to bond-forming reactions in the F–T process.<sup>12</sup>

Bercaw's contribution to the logic of the F–T process was significant. The research provided the first clear examples of C–H and C–C bond-forming reactions derived from transition metal complexes prepared from dihydrogen and carbon monoxide and were in stark contrast to “reagent-based” model systems. Although the modeling of the F–T process by early transition metal model systems was still occasionally questioned, the variety of bond-forming processes found and vetted via pertinent reactions was not.

### 3. METALLOCENE-CATALYZED ALKENE POLYMERIZATION

John Bercaw's long-standing interests in metallocene chemistry coupled with his desire to understand fundamental organometallic transformations made his transition into metallocene-catalyzed alkene polymerization catalysis both natural and seamless. Early studies focused on understanding olefin insertion into metal–hydrogen and metal–carbon bonds, the key initiation and propagation steps in the polymerization sequence. The microscopic reverse of alkene insertion into a metal–hydrogen bond,  $\beta$ -hydrogen elimination, is also an important chain transfer process. Despite the importance and ubiquity of these fundamental transformations, few detailed

mechanistic studies had been performed up to that point. Key questions such as the nature of the transition state, the influence of alkene electronic effects, metal identity, and cyclopentadienyl substitution all motivated these studies. In addition to fundamental insights, understanding the relative rates of these processes led to the development of catalysts that are tailored to produce polymers with the desired molecular weight.

Using the venerable bis(pentamethyl) cyclopentadienyl platform, niobocene<sup>13</sup> and tantalocene<sup>14</sup> olefin hydride complexes were synthesized as analogs for intermediates during catalysis. Both coalescence and magnetization transfer NMR experiments were used to measure the kinetics of alkene insertion. Within the family of group 5 metallocene olefin hydride complexes,  $(\eta^5\text{-C}_5\text{R}_5)_2\text{M}(\eta^2\text{-CH}_2=\text{CHR}')\text{H}$  ( $\text{M} = \text{Nb}$ ,  $\text{Ta}$ ;  $\text{R} = \text{H}$ ,  $\text{CH}_3$ ;  $\text{R}' = \text{H}$ ,  $\text{CH}_3$ ,  $\text{C}_6\text{H}_5$ ), ethylene insertion proved faster for less congested  $[\eta^5\text{-C}_5\text{H}_5]$  ligands relative to  $[\eta^5\text{-C}_5\text{Me}_5]$ . Similar effects were observed with propylene and styrene hydride compounds. Linear free energy relationships were examined with the styrene compounds, and a modestly polar transition structure was established with the migrating hydride bearing partial negative charge and the incipient carbon bearing partial positive charge (Figure 2).

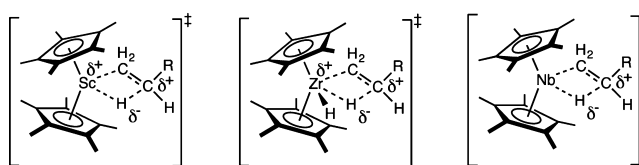


**Figure 2.** Transition structures established for alkene insertion and  $\beta$ -H elimination with scandocene, zirconocene, and niobocene complexes.

The transition state is stabilized when R is an electron-donating group; on the other hand, the ground state olefin complex is also stabilized when R is electron-withdrawing due to backbonding from the metal center. The niobocene complexes underwent faster insertion than the tantalum congeners, which can also be rationalized by viewing the insertion process as a reductive elimination because the  $\text{M}(\text{V})$ ,  $d^0$  resonance structure is likely quite important. The third row transition metal, seeking to maintain its highest oxidation is reticent to undergo reductive elimination, and hence, faster rates are observed with Nb.

The use of isolable group 5 metallocene olefin hydrides as mimics of insertion intermediates was revisited to gain insight into the impact of an ansa bridge on rates of insertion and alkene coordination preferences in stereochemically rigid metallocenes. Working in collaboration with long-time friends and colleagues, Malcolm and Jennifer Green, it was found that singly  $[\text{Me}_2\text{Si}]$ -bridged *ansa*-niobocenes underwent intramolecular hydrogen exchange 3 orders of magnitude faster than unbridged analogs.<sup>15</sup> Little rate enhancement was observed upon introduction of a second  $[\text{Me}_2\text{Si}]$  bridge. The origin of this effect was elucidated using DFT calculations, which suggested the electron population shifts from the ground state to the transition state most favorably for the singly bridged  $[\text{Me}_2\text{Si}]$  complex.

Much like his Ph.D. studies with H. H. Brintzinger in reduced titanium chemistry, John and his research group used the  $[\eta^5\text{-C}_5\text{Me}_5]$  ligand to pioneer the organometallic chemistry of scandium.<sup>16</sup> This chemistry extended well beyond synthesis:

access to well-defined organoscandocenes enabled fundamental studies into some of the most basic and important transformations in organometallic chemistry. Experiments with the scandocene alkyl complexes  $\text{Cp}^*_2\text{ScCH}_2\text{CH}_2\text{R}$  resulted in elucidation of the transition structure for  $\beta$ -hydrogen elimination (Figure 2). By trapping the putative scandocene hydride with 2-butyne, the rate constants for  $\beta$ -H elimination were determined as a function of alkyl substituent.<sup>17</sup> As with the group 5 metallocene chemistry, linear free energy relationships were consistent with positive charge accumulation at the  $\beta$ -carbon, meaning that hydride ( $\text{H}^{\delta-}$ ) is transferred to the electropositive metal.

Because most metallocene polymerization catalysts are based on group 4 metals,<sup>18</sup> later efforts were devoted to understanding insertion and  $\beta$ -H elimination with Zr and Hf compounds. An additional motivation was to understand why metallocene polymerization catalysts were extremely active for ethylene and  $\alpha$ -olefin polymerization but internal and 1,1-disubstituted alkenes proved largely unreactive. Using the hafnocene dihydride  $\text{Cp}^*_2\text{HfH}_2$ ,<sup>19</sup> the relative rates of insertion were found to be 1-pentene > styrene  $\gg$  *cis*-2-butene > cyclopentene > *trans*-2-butene > isobutene.<sup>20</sup> Determination of the rate constants for isobutene insertion with different zirconocenes revealed the pronounced effect of cyclopentadienyl substitution. Simply removing one methyl group from  $\text{Cp}^*_2\text{ZrH}_2$  to  $(\eta^5\text{-C}_5\text{Me}_5)(\eta^5\text{-C}_5\text{Me}_4\text{H})\text{ZrH}_2$  resulted in a  $3.8 \times 10^3$  rate enhancement at  $-63^\circ\text{C}$ . Primary kinetic deuterium isotope effects coupled with a linear free energy correlation to  $\sigma$  with  $\rho = -0.46(1)$  for insertion of substituted styrenes support rate-determining hydride transfer to coordinated olefin with small positive charge buildup at the  $\beta$ -carbon of the inserting styrene, analogous to the scandium and group 5 examples (Figure 2). The zirconocene alkylhydride products allowed the measurement of  $\beta$ -hydrogen elimination rate constants as a function of alkyl substituent and cyclopentadienyl rings. Equilibration of various alkyls permitted free energy profiles to be constructed for both insertion and  $\beta$ -hydrogen elimination for each alkene (Figure 3).

Having gained a comprehensive understanding of both the olefin insertion and  $\beta$ -hydrogen elimination transition structures with metallocenes of groups 3–5, attention was devoted to catalytic alkene polymerization. It was long suspected that formally 14-electron metallocenium alkyl cations with weakly coordinating anions were the propagating species responsible for chain growth.<sup>21</sup> Efforts in the Bercaw group were initially devoted to the discovery of “single component” catalysts: those that did not require large excesses of alkyl aluminums for activity. Permethylscandocene complexes were ideal for this purpose because the compounds are monomeric and the chemistry is predictably confined to the metallocene wedge where the frontier molecular orbitals are located.<sup>22</sup> The rate constants for ethylene insertion into various  $\text{Cp}^*_2\text{ScR}$  (R = alkyl, aryl) complexes were measured with the value for the ethyl derivative being particularly sluggish because of a  $\beta$ -agostic C–H interaction in the ground state.<sup>17</sup> With the scandocene propyl complex,  $(\eta^5\text{-C}_5\text{Me}_5)_2\text{ScCH}_2\text{CH}_2\text{CH}_3$ , living polymerization of ethylene was observed at  $-80^\circ\text{C}$ , representing one of the first single component catalysts for this transformation. Attempts to polymerize higher alkenes such as propylene resulted in C–H activation via  $\sigma$ -bond metathesis, a consequence of the congested metallocene steric environment that likely prevents coordination of the olefin  $\pi$ -bond, thus making vinylic C–H activation the preferred outcome.

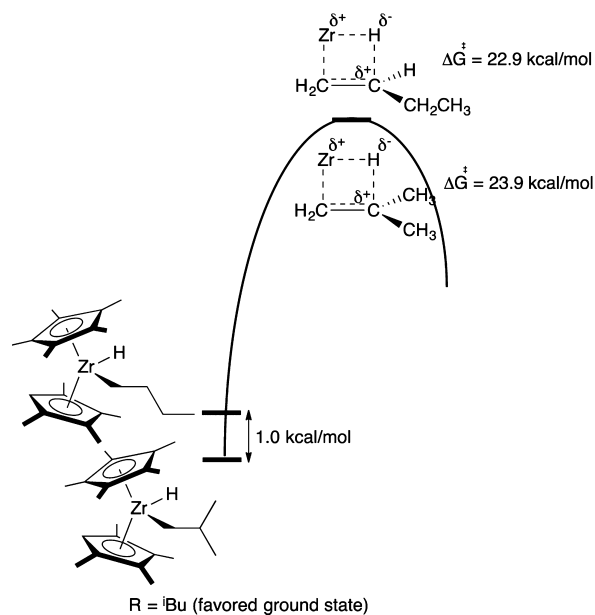


**Figure 3.** Free energy profiles for  $\beta$ -H elimination for zirconocene alkylhydride complexes showing relative ground state and transition state energies.

To relieve some of the steric congestion and open the coordination sphere of the metal to promote  $\alpha$ -olefin insertion, *ansa*-scandocenes bridged by  $[\text{Me}_2\text{Si}]$ -linkers were synthesized. This approach sacrifices some of the simplicity of the  $[\text{Cp}^*_2\text{Sc}]$  platform because dimeric or phosphine-stabilized hydrides are the isolable precursors.

Both  $[\text{Me}_2\text{Si}(\eta^5\text{-C}_5\text{Me}_4)_2]\text{Sc}(\text{H})(\text{PMe}_3)$  (“Op”) and *meso*- $[\text{Me}_2\text{Si}(\eta^5\text{-C}_5\text{H}_3\text{-3-}^i\text{Bu})_2]$  (“Dp”) were active for the catalytic dimerization of terminal olefins, with the former being more active (Figure 4).<sup>23</sup> Selective “head-to-tail” dimerization was observed in all cases. Catalytic cyclizations of  $\alpha,\omega$ -dienes to form the corresponding methylenecycloalkanes in high yield under mild conditions proved to be a useful extension of this reactivity.<sup>16b</sup> Various group 3 metallocene and lanthanide catalysts have since been developed for medium ring synthesis,

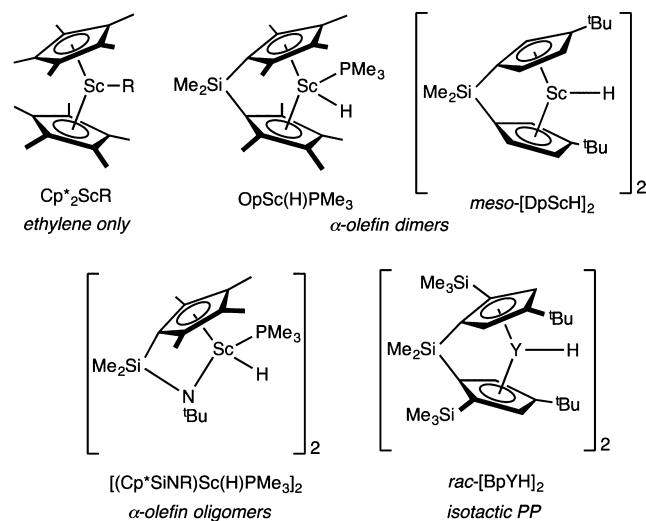


**Figure 4.** Evolution of single component, scandocene, and yttrrocene alkene polymerization catalysts.

and the cyclization reactions have been coupled to termination by hydrogenation, silylation, and boration.<sup>24</sup>

The observation of facile and selective hydrogenative cyclization of  $\alpha,\omega$ -dienes to methyl cycloalkanes allowed the Bercaw group to answer a long-standing question about the nature of the transition structure in metallocene-catalyzed alkene polymerization. Consensus had been established that the doubly coordinatively unsaturated, 14-electron metallocene alkyls (or alkyl cations) were required for propagation, but the origin of this requirement and the geometry of the olefin insertion transition state remained open questions. The modified “Green–Rooney” mechanism invoked coordination of a C–H bond to assist and lower barriers for olefin insertion<sup>25,26</sup> and possibly influence the stereochemical outcome.<sup>27</sup> Grubbs and co-workers<sup>28</sup> designed a clever deuterium labeling experiment to probe for an  $\alpha$ -agostic interaction for the cyclization of *rac*-1-*d*<sub>1</sub>-5-hexenylchlorotitanocene following activation with AlCl<sub>3</sub>Et<sub>2</sub> at –100 °C. Analysis of the resulting *cis*- and *trans*-2-*d*<sub>1</sub>-cyclopentylmethyl stereoisomers revealed a 1.00 ± 0.05 ratio of products, arguing against an  $\alpha$ -agostic interaction. Using OpSc(H)(PMe<sub>3</sub>)<sub>3</sub>, Piers and Bercaw<sup>29</sup> carried out the hydrogenative cyclization of *trans,trans*-1,6-*d*<sub>2</sub>-1,5-hexadiene, and <sup>2</sup>H NMR spectroscopy established a (1.19 ± 0.04):1 ratio of *trans*/*cis* products. The isotopic perturbation of stereochemistry is a result of an  $\alpha$ -agostic interaction in the transition structure, and the preference for H over D to occupy this bridging position leads to an excess of the *R,R* (*trans*) product. These results provided the first experimental evidence for the apparent requirement for active catalysts to be 14-electron metallocene alkyl derivatives with two vacant orbitals: one to accommodate the incoming olefin, the other to accommodate the  $\alpha$ -agostic interaction. This view of the transition structure has been corroborated with other metallocenes in both cyclization and  $\alpha$ -olefin dimerization reactions.<sup>30</sup>

The promising reactivity of the *ansa*-scandocenes along with the reasoning that more open metallocenes would favor alkene insertion rather than chain transfer inspired the preparation of even more open and potentially more reactive compounds. Further progression in ligand design resulted in replacement of one of the cyclopentadienyl ligands with an amido group, giving rise to the famous “[Cp\*SiNR]” class of compounds. The extreme Lewis acidity of the lower electron count scandium is evident in the synthetic chemistry because hydrogenation of the sterically protected alkyl complex, [Me<sub>2</sub>Si( $\eta^5$ -C<sub>5</sub>Me<sub>4</sub>)(<sup>t</sup>BuN)-ScCH(SiMe<sub>3</sub>)<sub>2</sub>] in the presence of PMe<sub>3</sub> yielded the dimeric, base-stabilized hydride [Me<sub>2</sub>Si( $\eta^5$ -C<sub>5</sub>Me<sub>4</sub>)(<sup>t</sup>BuN)Sc(H)(PMe<sub>3</sub>)<sub>2</sub>].<sup>31,32</sup> Notably, this compound was active for the oligomerization of  $\alpha$ -olefins and furnished atactic products resulting from selective head-to-tail insertions.<sup>32</sup> This ligand architecture ultimately revolutionized the field of Ziegler–Natta polymerization catalysis, as several industrial patents were filed shortly after the Bercaw disclosure.<sup>33</sup> Titanium derivatives were commercialized and became the basis for Dow’s INSITE catalyst technology, a process responsible for over 1 billion pounds of polyolefins and elastomers each year.<sup>34</sup>

The Bercaw group’s interests in metallocene-catalyzed Ziegler–Natta polymerization extended beyond the preparation of single component catalysts and focused on the more challenging topic of understanding the origin of stereocontrol in  $\alpha$ -olefin polymerization. C<sub>2</sub> symmetric metallocenes have emerged as some of the most active regio- and stereoselective catalysts known in all of catalysis. One challenge in synthesizing

the desired C<sub>2</sub> diastereomer of the metallocene catalyst was separation from the unwanted meso isomer that often yields atactic polymer. The Bercaw group synthesized a new *ansa* cyclopentadienyl ligand, [Me<sub>2</sub>Si(2-SiMe<sub>3</sub>-4-<sup>t</sup>Bu-C<sub>5</sub>H<sub>2</sub>)<sub>2</sub>] (Bp) designed to metalate and yield only the desired *rac*, C<sub>2</sub> symmetric diastereomer.<sup>35</sup> The ytrocene hydride dimer, *rac*-[BpYH]<sub>2</sub> proved active for the isospecific polymerization of propylene, 1-butene, and 1-hexene. Melting temperatures and <sup>13</sup>C NMR analysis established a very high isospecificity, allowing a more detailed understanding of how the steric environment governs the remarkably high stereoselectivities.

Adroit ligand design was again used to prepare single enantiomer catalysts by direct metalation rather than by the traditional method of resolution of the *rac* diastereomers.<sup>36</sup> Use of a stereogenic binaphthyl linking group in the *ansa*-silyl bridge cleanly yielded a single diastereomer ytrocene, demonstrating the concept of a “self resolving” ligand system and opening a straightforward pathway to enantiopure catalysts.<sup>37</sup> This synthetic advance provided the necessary precursors and allowed direct measure of the enantioselectivity of alkene insertion into metal–hydride and alkyl bonds.<sup>38</sup> Using a specifically deuterium-labeled 1-pentene and the enantiopure ytrocenes, Gilchrist and Bercaw determined that the insertion into the M–H hydride proceeded with a modest enantioselectivity of 34% ee, whereas insertion into the yttrium alkyl was highly selective (>40:1) (Figure 5).<sup>39</sup> Importantly,

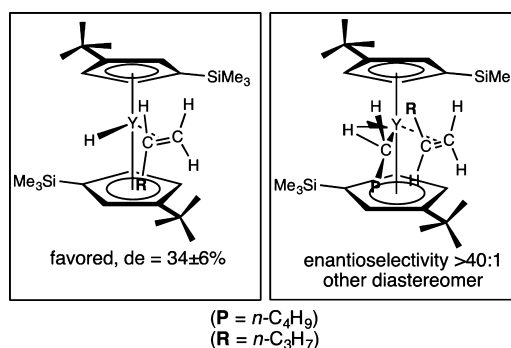
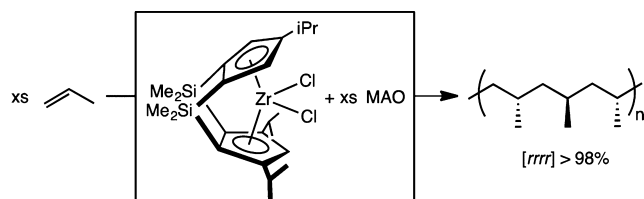


**Figure 5.** Stereoselectivity of pentene insertion into ytrocene hydrides (left) vs ytrocene alkyls (right).

this study established the definitive stereochemical model for isospecific  $\alpha$ -olefin polymerization and revealed that a *trans* relationship between the metal–alkyl and incoming alkene was the dominant discriminating steric interaction and that the chirality of the C<sub>2</sub> symmetric metallocene is transmitted indirectly to the incoming olefin.

The definitive experimental identification of  $\alpha$ -agostic assistance, in conjunction with the elucidation of the origin of enantiofacial discrimination in the transition structure for C–C insertion in isospecific polymerization catalysts provided the Bercaw group with a blueprint for the rational design of catalysts with potentially more sophisticated levels of stereocontrol. The syndiospecific polymerization of propylene is one such target because the catalyst must perfectly alternate between enantiotopic sides to generate alternating stereocontrol.<sup>40</sup> Application of these various mechanistic principles allowed the Bercaw team to design new doubly [SiMe<sub>2</sub>]-bridged bis(cyclopentadienyl) ligands (Scheme 4).<sup>41</sup> Activation of C<sub>2</sub> symmetric zirconocene dichlorides with MAO produced highly active, syndiospecific catalysts for the polymerization of

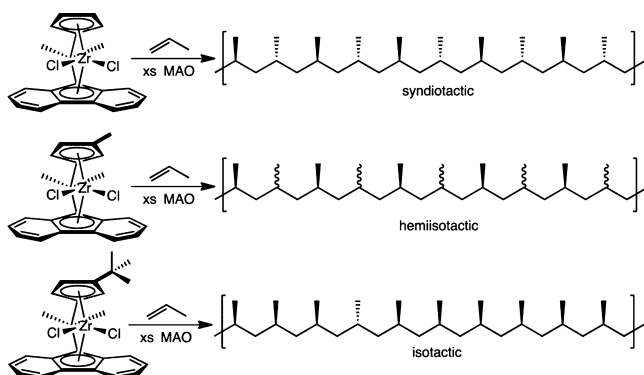
#### Scheme 4. Application of Doubly [SiMe<sub>2</sub>]-Bridged *ansa*-Zirconocene Catalysts to Syndiospecific Propylene Polymerization



propene; *rrrr* pentad content was 98.9% in optimal cases. Mechanistic studies<sup>42</sup> explored the influence of cyclopentadienyl substituents, monomer concentration, and isotopologues of propylene on the stereospecificity of the propylene polymerization reaction. The microstructures of the polymers, determined by <sup>13</sup>C NMR spectroscopy, were consistent with stereocontrol dominated by site epimerization, where an inversion of configuration at the zirconium results from the polymer swinging from one side of the metallocene wedge to the other without monomer insertion. The high activity of the doubly [SiMe<sub>2</sub>]-bridged zirconocenes was exploited for the polymerization of olefins that are typically challenging for more classical catalysts.<sup>43</sup> Terminal olefins with bulky substituents in the 3- or 4-positions were readily polymerized, and introduction of chiral alkyl substituents on the cyclopentadienyl rings enabled the kinetic resolution polymerization of racemic monomers. In one case, the polymerization of 3,4-dimethyl-1-pentene, high kinetic selectivity (*s* > 15) was observed.

The Bercaw model for stereochemical control was also extended to the design of new zirconocene catalysts to produce unique polymer architectures (Scheme 5). Preparation of C<sub>1</sub>-

#### Scheme 5. New Polymer Architectures Accessed from Rational Manipulation of Ligand Substituents of Cyclopentadienyl-Fluorenyl Zirconocene Catalysts



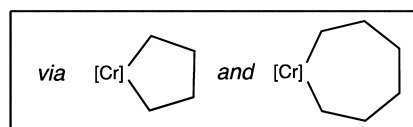
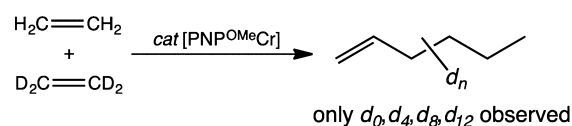
symmetric variants of “Ewen–Razavi”-type<sup>44</sup> cyclopentadienyl-fluorenyl zirconium complexes with large cyclopentadienyl substituents influenced polymer architecture, and the linker between the two rings determined polymer molecular weight.<sup>45</sup> Catalyst systems resulting from this structural fine-tuning yielded elastomeric polypropylene having an isotactic–hemiisotactic structure. Additional modification of the metallocene architecture by introduction of sterically expansive fluorenyl ligands with mono- and bis(tetramethylhydrobenzo) substituents afforded catalysts that generated highly stereoregular syndiotactic polypropylene with melting temperatures as high as 153 °C.<sup>46</sup>

The origin of stereospecificity of certain types of C<sub>1</sub>-symmetric cyclopentadienyl-fluorenyl catalysts was also examined by polymer microstructure analysis, monomer pressure effects and temperature.<sup>47</sup> An alternating mechanism was favored in which both sides of the metallocene wedge are utilized for insertion. The observation of higher isotacticity at higher polymerization temperatures and lower monomer concentrations supports a competitive site epimerization (inversion at Zr) pathway.

As the Bercaw group moved into the 21st century, catalysts for alkene polymerization transitioned into the “post-metallocene” era.<sup>48</sup> Group 3 chemistry focused on the chemistry of tetradentate, monoanionic, phenol-based ligands that supported modestly active metal dialkyl complexes for the polymerization of ethylene.<sup>49</sup> Other platforms included “LX<sub>2</sub>-type” bis(phenolate) chelates with neutral furan, thiophene, and pyridine donors and their corresponding group 4 metal complexes.<sup>50</sup> Bis(phenolate) derivatives of Ti, Zr, Hf, and V<sup>51</sup> as well as C<sub>2</sub>-symmetric titanium and zirconium bis(anilide)-pyridine complexes were also synthesized. Each of these new compounds exhibits low activity and selectivity in propylene polymerization.<sup>52</sup> Other nonmetallocene complexes supported by bis(thiophenolate)pyridine,<sup>53</sup> modular anilide(pyridine)-phenoxide,<sup>54,55</sup> and bis(phosphido) pyridine<sup>56</sup> ligands were also evaluated in catalytic alkene polymerization.

During this time, Bercaw and his group expanded their interests in understanding the mechanism of selective ethylene trimerization promoted by (PNP<sup>OMe</sup>)Cr (PNP<sup>OMe</sup> = (*o*-MeO-C<sub>6</sub>H<sub>4</sub>)<sub>2</sub>PN(Me)P(*o*-MeO-C<sub>6</sub>H<sub>4</sub>)<sub>2</sub>) compounds activated with MAO.<sup>57</sup> One mechanistic proposal invoked metalocyclic intermediates over a traditional Cossee-type mechanism to account for the selectivity of C<sub>6</sub> products, although no direct experimental support had been provided. In a quintessential Bercaw–Jay Labinger study,<sup>58</sup> a clever isotopic labeling study was devised whereby a 1:1 mixture of C<sub>2</sub>D<sub>4</sub> and C<sub>2</sub>H<sub>4</sub> was trimerized upon activation of well-defined organometallic chromium complexes. Analysis of the isotopologues of the 1-hexene product revealed no isotopic scrambling because only C<sub>6</sub>D<sub>12</sub>, C<sub>6</sub>D<sub>8</sub>H<sub>4</sub>, C<sub>6</sub>D<sub>4</sub>H<sub>8</sub>, and C<sub>6</sub>H<sub>12</sub> products were observed in a 1:3:3:1 ratio, consistent with a metalocyclic rather than Cossee-type pathway (Scheme 6). Trimerization of 1,1-d<sub>2</sub>-

#### Scheme 6. Chromium-Catalyzed Trimerization of a 1:1 Mixture of C<sub>2</sub>H<sub>4</sub> and C<sub>2</sub>D<sub>4</sub> Supporting a Metalocyclic Pathway



ethylene established a kinetic isotope effect of 1.3 (298 K), distinct from the value of 2.4 measured in the previous experiment, consistent with irreversible formation of a symmetric metalocycloheptane. Subsequent studies focused on evaluation of ancillary ligand effects as well as detailed studies of the catalyst activation mode and determination of the number of active chromium compounds.<sup>59,60</sup> These studies

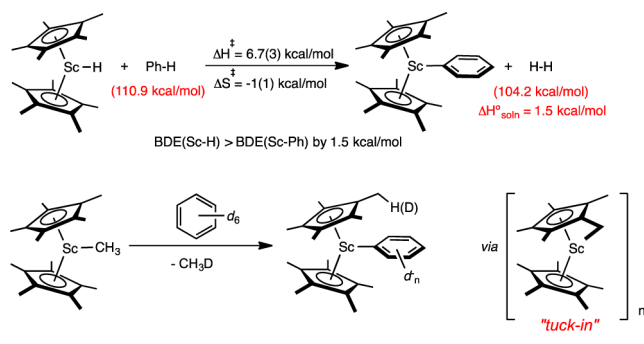
were also extended to explore the activity and selectivity of phenoxyimine titanium trimerization catalysts.<sup>61</sup>

#### 4. C–H AND C–C ACTIVATIONS

Until Crabtree<sup>62</sup> and Ephritikhine<sup>63</sup> provided examples of homogeneous  $sp^3$ -carbon–hydrogen bond activations by transition metals, and Bergman<sup>64</sup> discovered a discrete oxidative addition of the CH bond of cyclohexane, the reactivity of RH was limited to free-radical processes. Typically observed in the context of autoxidation,<sup>65</sup> free radical activations show a pronounced lack of selectivity, principally because the first products of autoxidation are more susceptible to further reactivity than the initial substrate. The fundamental surprise of metal-based C–H activations was their correlation with the *strength* of the R–H bond,<sup>66,67</sup> which is in stark contrast to free radical reactions, whose reactivity in inversely correlated with substrate BDE (bond dissociation enthalpy).

Bercaw's contributions to CH-bond activation initiated through studies of electrophilic, early metal systems in which highly substituted cyclopentadienyl rings were prominent features. In the earliest investigation, Bercaw took advantage of his knowledge of four-center transition states attributed to  $d^0$  systems, especially the concept of  $\sigma$ -bond metathesis,<sup>68</sup> whose origins derived in part from chemistry discovered by his Ph.D. advisor, Hans Brintzinger.<sup>69,70</sup> In Scheme 7, the hydrogenation

**Scheme 7. Application of  $Cp^*_2ScR$  Compounds to C–H Bond Activation**



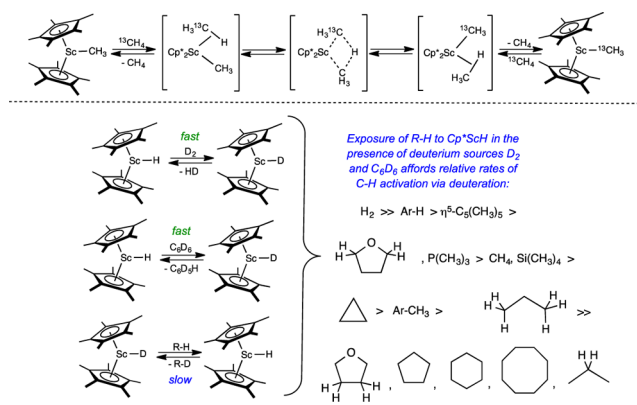
of scandium alkyls (R) as  $Cp^*_2ScR$  led to the extraordinarily reactive hydride  $[Cp^*_2ScH]_n$ , which was stable only under dihydrogen (>1 atm) yet isolable as a THF adduct,  $Cp^*_2ScH \cdot (THF)$ . Because hydrogenolysis was an effective means of Sc–R bond scission, the reverse was likely to be observable in cases that the  $D(Sc-R)$  approached that of  $D(Sc-H)$ . The phenyl derivative,  $Cp^*_2ScPh$ , proved to possess a  $D(Sc-Ph)$  of strength comparable to that of the scandium–hydride bond, as equilibrium studies indicated. As in other cases of nonradical C–H bond activation,  $\Delta S^\ddagger$  values obtained in such measurements were small, and the relative free energies were within error of the relative enthalpies ( $\Delta \Delta G^\ddagger \sim \Delta \Delta H^\ddagger$ ).

As shown for the case of  $Cp^*_2ScCH_3$ , thermolysis of scandium alkyls in benzene- $d_6$  ultimately afforded the  $d_5$ -phenyl derivative  $Cp^*_2ScC_6D_5$ , albeit with some deuterium scrambled into the methyl groups of the pentamethylcyclopentadienyl ligand due to the partial involvement of a "tuck-in" complex. In either path,  $\sigma$ -bond metathesis steps swapped ScR for ScR' bonds, revealing C–H bond activation akin to that of the hydride.

The initial  $\sigma$ -bond metathesis results were augmented by the "self-metathesis" of methane, observed via the exchange of

$^{13}CH_4$  with the methyl of  $Cp^*_2ScCH_3$ , and a series of deuteration studies that permitted the relative activation rates of a variety of hydrocarbons, as illustrated in Scheme 8. The

**Scheme 8. Isotopic Labeling Experiments with Relevance to C–H Activation by  $Cp^*_2ScR$  Complexes**

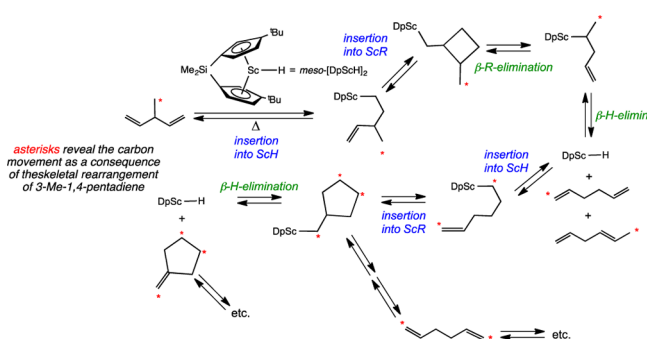


trend of relative C–H bond activations is typical of nonradical, concerted  $2e^-$  processes observed in oxidative addition, 1,2-RH-addition, and  $\sigma$ -bond metathesis processes. The reactivity correlates with the strength of the Sc–C bond formed; hence,  $sp^2$  CH bonds are favored over primary, secondary, and tertiary (not observed)  $sp^3$  CH bonds. Deviations are observed for species containing heteroatoms that can bind to the  $14 e^-$   $Cp^*_2ScR$  center, where the proximity of the substrate CH bond to the Sc(R/H) group lowers the barrier to activation. Central to this rationale is the understanding that the differences in scandium–hydrocarbonyl bond enthalpies are greater than the differences in the corresponding carbon–hydrogen bond enthalpies (i.e.,  $\Delta D(Sc-R) > \Delta D(R-H)$ ).

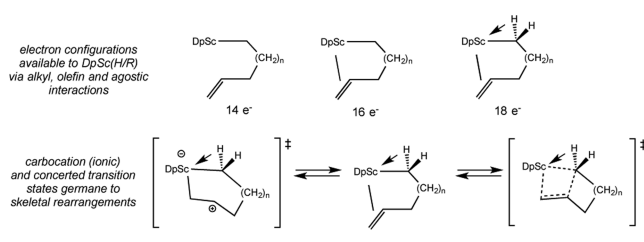
In conjunction with the carbon–hydrogen bond activation studies, skeletal rearrangements of hydrocarbons were observed within a related system, and the extreme electrophilicity of unsaturated scandium organometallic complexes proved to be the key property. An enhancement in electrophilicity over  $Cp^*_2ScH$  was achieved via the implementation of the *ansa*-bis(<sup>t</sup>Bu-cyclopentadienyl) ligand, Dp, as in the hydride complex  $DpScH$ . In addition to common processes, that is,  $\beta$ -H-elimination and olefin insertion into the scandium hydride, the  $14 e^-$  scandium center mediated related  $\beta$ -alkyl-elimination events and olefin insertions into scandium alkyls.<sup>23</sup> As Scheme 9 illustrates, these *reversible* steps combine to mediate the scrambling of carbons in diene substrates and provide the means for hydrocarbon rearrangements.

While turning pure materials into mixtures is typically not productive, the examples provided by Bercaw encompassed numerous fundamental steps pertinent to olefin oligomerization, polymerization, and related electrophilic reactions. The homogeneous skeletal rearrangements provided a landscape upon which the heterogeneous reforming of hydrocarbons could be viewed. As a fundamental study, the work is unparalleled in revealing the capabilities of electrophilic early transition metals as Lewis acid alternatives to homogeneous or heterogeneous Bronsted acid catalysts. Scheme 10 illustrates increasing the electron count of the  $14 e^-$   $DpScR$  center via olefin binding ( $16 e^-$ ) and the agostic interaction of the alpha hydrogens ( $18 e^-$ ). Through seminal kinetic isotope effect studies on cyclizations of the type shown in Scheme 9,<sup>29</sup> Bercaw showed that the agostic interaction and, by inference,

### Scheme 9. Hydrocarbon Rearrangements Promoted by DpScR Complexes



### Scheme 10. Olefin Insertion into Sc–R Bonds Highlighting the Importance of Agostic Interactions



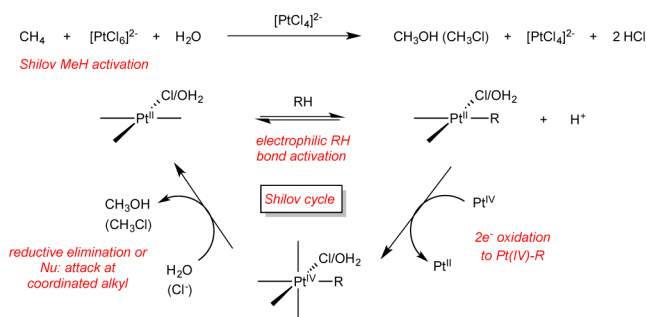
the initial 14  $e^-$  center are necessary for swift, reversible olefin insertions into the scandium-alkyl bond.

Two mechanistic extremes may be considered in regard to the olefin insertion process characterized by ionic and concerted transition states. Given the extreme electrophilicity of the scandium center, it is likely that substantial charge build-up occurs within a generally concerted insertion event.

### 5. REVISITING SHILOV HYDROCARBON OXIDATION

As the number of CH-bond activating systems grew,<sup>71</sup> the problem morphed into making such events productive. A Holy Grail in organometallic chemistry is the *direct* conversion of hydrocarbon feedstocks into commodity chemicals, a process that encompasses the selective activation of an alkane and its functionalization. Bercaw's interest in this potentially transformative conversion<sup>72</sup> led him in pursuit of Shilov chemistry<sup>73</sup> and its mechanism, shown in Scheme 11. Bercaw's signature approach of isolating and analyzing each plausible step helped solidify and detail this process and opened up new avenues for late metal hydrocarbon activation. This program also involved a highly productive collaboration with Jay Labinger, John's colleague in the Beckman Institute at Caltech. Although this

### Scheme 11. Shilov RH Activation Reaction and Likely Cycle

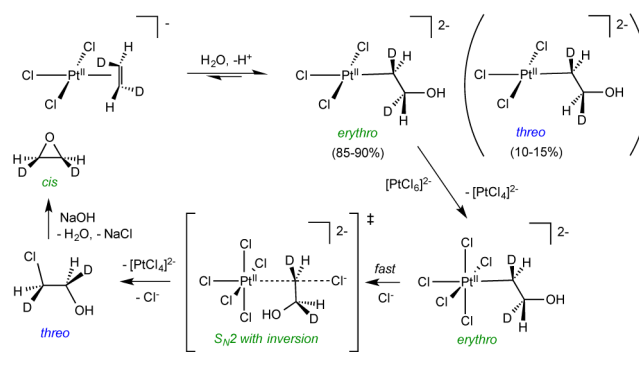


Account focuses on the contributions of the Bercaw group, Labinger's contributions proved invaluable, and he served as a coadvisor for many in the Bercaw laboratory.

The aqueous process<sup>72,74,75</sup> may be separated into three critical steps: (1) the activation of RH by Pt(II) to form a Pt(II) alkyl and a proton; (2) the 2  $e^-$  oxidation of the Pt(II)-R species to afford the corresponding Pt(IV) alkyl; and (3) a reductive process involving an elimination of ROH (RCl) or a related external nucleophilic attack to give the same products. Note that the charge balance in each step (Scheme 11) is dependent on the amount of chloride vs water in the coordination sphere about Pt, but the two protons released in the process are ultimately balanced by chlorides.

Perhaps the most intriguing step of the process is the product-forming step, because an ambiguity between reductive elimination or an external nucleophilic attack persisted. In addition to conducting kinetics experiments that were consistent with  $\text{CH}_3\text{X}$  (X = OH, Cl) formation from either six- or five-coordinate intermediates, Bercaw devised an elegant labeling experiment to differentiate the path of reduction.<sup>76,77</sup> Isolation of the Pt(IV) alkyl had proven elusive because of rapid degradative protonation and disproportionation events, thereby hampering stereochemical probes. The problem was cleverly bypassed via the oxidation of a transient  $\beta$ -hydroxyethyl species prepared via nucleophilic attack by water on Zeise's salt. Use of *trans*-1,2-dideuterioethylene provided the stereochemical assay needed to discern the product-forming step, as Scheme 12

### Scheme 12. Stereochemical Interrogation of the Pt–C Bond Cleavage Reaction Revealing $\text{S}_{\text{N}}2$ Attack with Inversion



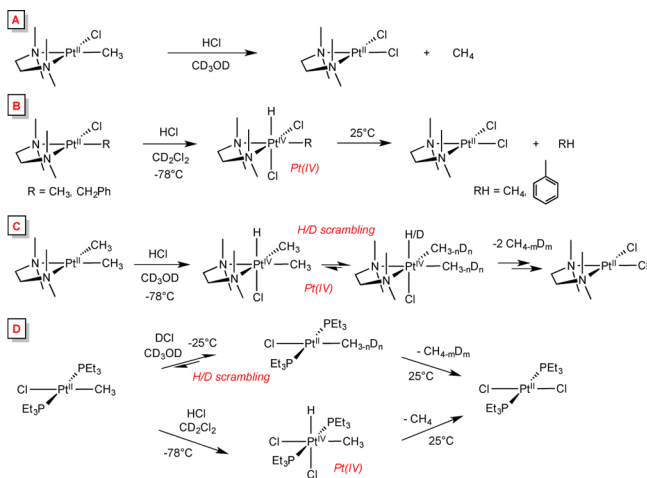
illustrates, since the erythro  $\beta$ -hydroxyethyl Pt(II) complex was generated in excess over its threo complement as a result of external attack by water. The subsequent oxidation by Pt(IV) in the presence of chloride afforded ClCHDCHDOH of unknown stereochemistry, but closure to its epoxide revealed a *cis* geometry. The product was thus inferred as *threo*-ClCHDCHDOH, which was likely derived from nucleophilic attack at the  $\alpha$ -carbon of the Pt(IV)  $\beta$ -hydroxyethyl intermediate.

In the Shilov systems, kinetics experiments were clearly consistent with the 2  $e^-$  Pt(IV) oxidation of the Pt(II) alkyl prior to reduction to products; hence, the hydrocarbon activation occurred via Pt(II). The mechanism of this activation was viewed as either (1) electrophilic attack of the R-H bond with concomitant deprotonation, or (2) oxidative addition of the R-H bond to afford a discrete Pt(IV) alkylhydride intermediate. In typical Bercaw fashion, the plausibility of an intermediate Pt(IV) complex was attacked by viewing its formation in reverse.<sup>74</sup>



Scheme 13 shows selected results from platinum alkyl protonation studies and illustrates the information gained by

### Scheme 13. Mechanistic Experiments Pertaining to the Shilov Reaction Utilizing the Principle of Microscopic Reversibility

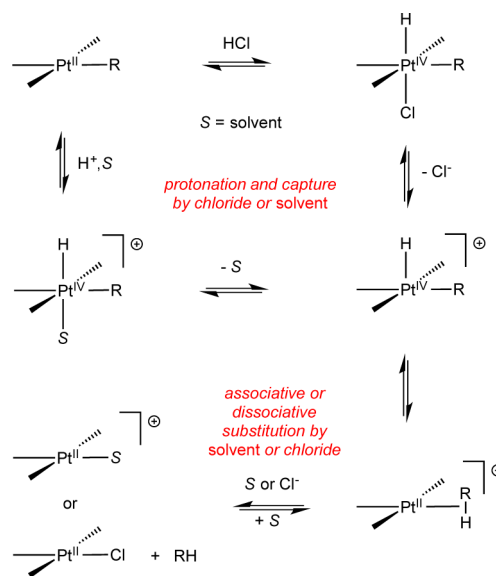


exploring reactions via the principle of microscopic reversibility. In part A, protonation of  $(\text{tmeda})\text{PtCl}(\text{CH}_3)$  ( $\text{tmeda} = \text{Me}_2\text{NCH}_2\text{CH}_2\text{NMe}_2$ ) afforded only the corresponding dichloride and methane in methanol, but a switch to  $\text{CD}_2\text{Cl}_2$  enabled low-temperature observation of Pt(IV) alkylhydride complexes prior to reductive elimination of RH upon warming (B). A change to  $(\text{tmeda})\text{Pt}(\text{CH}_3)_2$  not only revealed the related Pt(IV) dimethylhydride intermediate, but showed H/D scrambling with the  $\text{CD}_3\text{OD}$  solvent, a process implicating the intermediacy of alkane complexes (C). Solvents can also clearly affect the course of chemical reactivity (D), as the treatment of  $\text{trans}-(\text{Et}_3\text{P})_2\text{PtCl}(\text{CH}_3)$  with HCl (or DCl) in methanol affirms the intermediacy of alkane complexes via deuteration of the methyl substituents without evidence of a Pt(IV) species, whereas it is observable in methylene chloride.

Scheme 14 summarizes the mechanistic findings of Bercaw and co-workers about the critical RH activation step of the Shilov process, albeit described in reverse. Protonation of Pt(II) affords either the Pt(IV) solvated cation or the neutral HCl oxidative addition product, and loss of the solvent or chloride in the ensuing step provides the critical square pyramidal, five-coordinate alkylhydride cation. Reductive elimination to an alkane adduct without RH loss provides the means of H/D scrambling observed in Scheme 12 when considered in combination with reversible proton transfer events. The loss of alkane in either a dissociative or associative manner provides the product solvate or neutral chloride. The five-coordinate intermediate is crucial because it obviates orbital symmetry constraints of HR oxidative addition to square planar complexes, and the complementary HR reductive elimination from octahedral species. In the Shilov oxidation, substitution of water or  $\text{Cl}^-$  by RH affords the alkane complex, which then oxidatively adds reversibly, and the resulting five-coordinate alkylhydride is trapped by water or chloride.

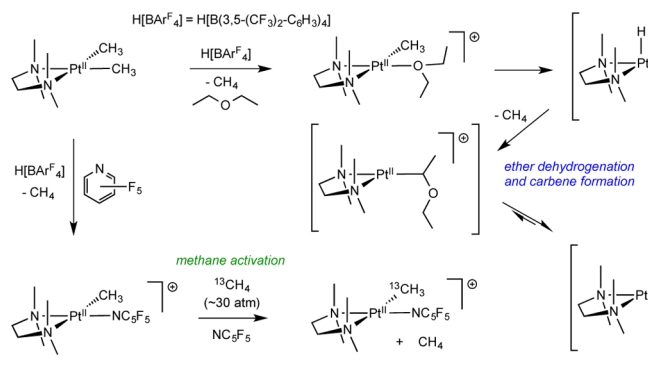
During the course of these studies, several groups investigated CH bond activations via electrophilic platinum and palladium centers, but the investigations of Bercaw show the relationship of aqueous Shilov chemistry to those involving nonaqueous environments<sup>78–80</sup> and provide the mechanistic

### Scheme 14. C–H Activation Step of the Shilov System Inferred from Various Mechanistic Experiments



underpinning for all. Consider Scheme 15, which features some examples of CH bond activation by the electrophilic Pt(II)

### Scheme 15. Shilov and Related CH Bond Activations by Electrophilic Platinum Centers



cationic center generated upon protonation of  $(\text{tmeda})\text{Pt}(\text{CH}_3)_2$  and loss of methane.<sup>81</sup> The cationic Pt(II) center is so reactive that solvents must be carefully chosen, as witnessed by activation of the bound ether in  $[(\text{tmeda})\text{Pt}(\text{CH}_3)(\text{OEt}_2)]^+$  to afford methane, followed by formation of an ethoxy-methyl carbene hydride, presumably via  $\alpha$ -elimination. A switch to perfluoropyridine as the solvent enabled methane activation to be observed via Pt–CH<sub>3</sub> exchange with <sup>13</sup>CH<sub>4</sub> to give  $[(\text{tmeda})\text{Pt}(\text{<sup>13</sup>CH}_3)(\text{NC}_5\text{F}_5)]^+$ . Both reactions suffice as elegant examples of intra- and intermolecular examples of CH bond activation by electrophilic late metal complexes.

## SUMMARY

John Bercaw has had a distinguished career with landmark contributions to some of the most prominent challenges in organometallic chemistry and catalysis and has been an inspiration to numerous co-workers. We wish him a happy 70th birthday and good health and happiness for many more.

## AUTHOR INFORMATION

## Corresponding Authors

\*E-mail: ptw2@cornell.edu.

\*E-mail: pchirik@princeton.edu.

## Notes

The authors declare no competing financial interest.

## ACKNOWLEDGMENTS

We thank Professor Mark Thompson (University of Southern California) for providing the image in Figure 1.

## REFERENCES

- (1) Schulz, H. *Appl. Catal. A – Gen.* **1999**, *186*, 3–12.
- (2) Wolczanski, P. T.; Bercaw, J. E. *Acc. Chem. Res.* **1980**, *13*, 121–127.
- (3) Manriquez, J. M.; McAlister, D. R.; Sanner, R. D.; Bercaw, J. E. *J. Am. Chem. Soc.* **1976**, *98*, 6733–6735.
- (4) Marsella, J. A.; Curtis, C. J.; Bercaw, J. E.; Caulton, K. G. *J. Am. Chem. Soc.* **1980**, *102*, 7244–7246.
- (5) Tatsumi, K.; Nakamura, A.; Hofmann, P.; Stauffert, P.; Hoffmann, R. *J. Am. Chem. Soc.* **1985**, *107*, 4440–4451.
- (6) (a) Hofmann, P.; Frede, M.; Stauffert, P.; Lasser, W.; Thewalt, U. *Angew. Chem., Int. Ed. Engl.* **1985**, *24*, 712–713. (b) Hofmann, P.; Stauffert, P.; Frede, M.; Tatsumi, K. *Chem. Ber.* **1989**, *122*, 1559–1577.
- (7) (a) Marsella, J. A.; Caulton, K. G. *J. Am. Chem. Soc.* **1980**, *102*, 1747–1748. (b) Marsella, J. A.; Huffman, J. C.; Folting, K.; Caulton, K. G. *Inorg. Chim. Acta* **1985**, *96*, 161–170.
- (8) Moore, E. J.; Straus, D. A.; Armantrout, J.; Santarsiero, B. D.; Grubbs, R. H.; Bercaw, J. E. *J. Am. Chem. Soc.* **1983**, *105*, 2068–2070.
- (9) Barger, P. T.; Santarsiero, B. D.; Armantrout, J.; Bercaw, J. E. *J. Am. Chem. Soc.* **1984**, *106*, 5178–5186.
- (10) Berry, D. H.; Bercaw, J. E.; Jircitano, A. J.; Mertes, K. B. *J. Am. Chem. Soc.* **1982**, *104*, 4712–4715.
- (11) Wolczanski, P. T.; Threlkel, R. S.; Bercaw, J. E. *J. Am. Chem. Soc.* **1979**, *101*, 218–220.
- (12) Threlkel, R. S.; Bercaw, J. E. *J. Am. Chem. Soc.* **1981**, *103*, 2650–2659.
- (13) Doherty, N. M.; Bercaw, J. E. *J. Am. Chem. Soc.* **1985**, *107*, 2670–2682.
- (14) Burger, B. J.; Santarsiero, B. D.; Trimmer, M. S.; Bercaw, J. E. *J. Am. Chem. Soc.* **1988**, *110*, 3134–3146.
- (15) Ackerman, L. J.; Green, M. L. H.; Green, J. C.; Bercaw, J. E. *Organometallics* **2003**, *22*, 188–194.
- (16) (a) Chirik, P. J.; Bercaw, J. E. In *The Metallocenes*; Togni, A., Halterman, R. L., Eds.; Wiley-VCH Publishers: New York, 1998; pp 111–148. (b) Piers, W. E.; Shapiro, P. J.; Bunel, E. E.; Bercaw, J. E. *Synlett* **1990**, 74–84.
- (17) Burger, B. J.; Thompson, M. E.; Cotter, W. D.; Bercaw, J. E. *J. Am. Chem. Soc.* **1990**, *112*, 1566–1577.
- (18) Brintzinger, H. H.; Fischer, D.; Mülhaupt, D.; Rieger, B.; Waymouth, R. M. *Angew. Chem., Int. Ed. Engl.* **1995**, *34*, 1143–1170.
- (19) Roddick, D. M.; Fryzuk, M. D.; Seidler, P. F.; Hillhouse, G. L.; Bercaw, J. E. *Organometallics* **1985**, *4*, 97–104.
- (20) Chirik, P. J.; Bercaw, J. E. *Organometallics* **2005**, *24*, 5407–5423.
- (21) Jordan, R. F. *Adv. Organomet. Chem.* **1991**, *32*, 325–387.
- (22) Lauher, J. W.; Hoffmann, R. *J. Am. Chem. Soc.* **1976**, *98*, 1729–1742.
- (23) Bunel, E.; Burger, B. J.; Bercaw, J. E. *J. Am. Chem. Soc.* **1988**, *110*, 976–978.
- (24) Molander, G. A.; Romero, J. A. C. *Chem. Rev.* **2002**, *102*, 2161–2185.
- (25) Brookhart, M.; Green, M. L. H. *J. Organomet. Chem.* **1983**, *250*, 395–408.
- (26) Prosenc, M. H.; Janiak, C.; Brintzinger, H. H. *Organometallics* **1992**, *11*, 4036–4041.
- (27) Röhl, W.; Brintzinger, H. H.; Rieger, B.; Zolk, R. *Angew. Chem., Int. Ed. Engl.* **1990**, *29*, 279–280.
- (28) Clawson, L.; Soto, J.; Buchwald, S. L.; Steigerwald, M. L.; Grubbs, R. J. *J. Am. Chem. Soc.* **1985**, *107*, 3377–3378.
- (29) Piers, W. E.; Bercaw, J. E. *J. Am. Chem. Soc.* **1990**, *112*, 9406–9407.
- (30) Grubbs, R. H.; Coates, G. W. *Acc. Chem. Res.* **1990**, *29*, 85–93.
- (31) Shapiro, P. J.; Bunel, E.; Schaefer, W. P.; Bercaw, J. E. *Organometallics* **1990**, *9*, 867–869.
- (32) Shapiro, P. J.; Cotter, W. D.; Schaefer, W. P.; Labinger, J. A.; Bercaw, J. E. *J. Am. Chem. Soc.* **1994**, *116*, 4623–4640.
- (33) (a) Canich, J. M. Eur. Patent 420436, 1991. (b) Canich, J. M.; Hlatky, G. G.; Turner, H. W. U.S. Patent 542 236, 1990. (c) Stevens, J. C.; Timmers, F. J.; Wilson, D. R.; Schmidt, G. F.; Nickias, P. N.; Rosen, R. K.; Knight, G. W.; Lai, S. Eur. Patent 416 815, 1990.
- (34) Thayer, A. M. *Chem. Eng. News*, Sept 11, 1995.
- (35) Coughlin, E. B.; Bercaw, J. E. *J. Am. Chem. Soc.* **1992**, *114*, 7606–7607.
- (36) Grossman, R. B.; Doyle, R. A.; Buchwald, S. L. *Organometallics* **1991**, *10*, 1501.
- (37) Mitchell, J. P.; Hajela, S.; Brookhart, S. K.; Hardcastle, K. I.; Henling, L. M.; Bercaw, J. E. *J. Am. Chem. Soc.* **1996**, *118*, 1045–1053.
- (38) Pino, P.; Galimberti, M. *J. Organomet. Chem.* **1989**, *370*, 1–7.
- (39) Gilchrist, J. H.; Bercaw, J. E. *J. Am. Chem. Soc.* **1996**, *118*, 12021–12028.
- (40) Ewen, J. A. *Macromol. Symp.* **1995**, *89*, 181–196.
- (41) Herzog, T. A.; Zubris, D. L.; Bercaw, J. E. *J. Am. Chem. Soc.* **1996**, *118*, 11988–11989.
- (42) Veghini, D.; Henling, L. M.; Burkhardt, T. J.; Bercaw, J. E. *J. Am. Chem. Soc.* **1999**, *121*, 564–573.
- (43) Baar, C. R.; Levy, C. J.; Min, E. Y.-J.; Henling, L. M.; Day, M. W.; Bercaw, J. E. *J. Am. Chem. Soc.* **2004**, *126*, 8216–8231.
- (44) Ewen, J. A.; Elder, M. J. *Makromol. Chem., Makromol. Symp.* **1993**, *66*, 179–190.
- (45) Miller, S. A.; Bercaw, J. E. *Organometallics* **2002**, *21*, 934–945.
- (46) Miller, S. A.; Bercaw, J. E. *Organometallics* **2004**, *23*, 1777–1789.
- (47) Miller, S. A.; Bercaw, J. E. *Organometallics* **2006**, *25*, 3576–3592.
- (48) Gibson, V. C.; Spitzmesser, *Chem. Rev.* **2002**, *103*, 283–316.
- (49) Marinescu, S. C.; Agapie, T.; Day, M. W.; Bercaw, J. E. *Organometallics* **2007**, *26*, 1178–1190.
- (50) Agapie, T.; Henling, L. M.; DiPasquale, A. G.; Rheingold, A. L.; Bercaw, J. E. *Organometallics* **2008**, *27*, 6245–6256.
- (51) Golisz, S. R.; Bercaw, J. E. *Macromolecules* **2009**, *42*, 8751–8762.
- (52) Tonks, I. A.; Tofan, D.; Weintrob, E. C.; Agapie, T.; Bercaw, J. E. *Organometallics* **2012**, *31*, 1965–1974.
- (53) Lenton, T. N.; VanderVelde, D. G.; Bercaw, J. E. *Organometallics* **2012**, *31*, 7492–7499.
- (54) Klet, R. C.; VanderVelde, D. G.; Labinger, J. A.; Bercaw, J. E. *Chem. Commun.* **2012**, *48*, 6657–6659.
- (55) Klet, R. C.; Theriault, C. N.; Klosin, J.; Labinger, J. A.; Bercaw, J. E. *Macromolecules* **2014**, *47*, 3317–3324.
- (56) Winston, M. S.; Bercaw, J. E. *Organometallics* **2010**, *29*, 6408–6416.
- (57) Carter, A.; Cohen, S. A.; Cooley, N. A.; Murphy, A.; Scutt, J.; Wass, D. F. *Chem. Commun.* **2002**, 858–859.
- (58) Agapie, T.; Schofer, S. J.; Labinger, J. A.; Bercaw, J. E. *J. Am. Chem. Soc.* **2004**, *126*, 1304–1305.
- (59) Schofer, S. J.; Day, M. W.; Henling, L. M.; Labinger, J. A.; Bercaw, J. E. *Organometallics* **2006**, *25*, 2743–2749.
- (60) Do, L. H.; Labinger, J. A.; Bercaw, J. E. *Organometallics* **2012**, *31*, 5143–5149.
- (61) Sattler, A.; Labinger, J. A.; Bercaw, J. E. *Organometallics* **2013**, *32*, 6899–6902.
- (62) (a) Crabtree, R. H.; Mihelcic, J. M.; Quirk, J. M. *J. Am. Chem. Soc.* **1979**, *101*, 7738–7740. (b) Crabtree, R. H.; Mellea, M. F.; Mihelcic, J. M.; Quirk, J. M. **1982**, *104*, 107–113.
- (63) (a) Baudry, D.; Ephritikhine, M.; Felkin, H. *J. Chem. Soc. Chem. Commun.* **1980**, 1243–1244. (b) Baudry, D.; Ephritikhine, M.; Felkin, H. *J. Chem. Soc. Chem. Commun.* **1982**, 1235–1236. (c) Baudry, D.; Ephritikhine, M.; Felkin, H. *J. Chem. Soc. Chem. Commun.* **1983**, 788–789.

- (64) Bergman, R. G.; Janowitz, A. H. *J. Am. Chem. Soc.* **1982**, *104*, 352–354.
- (65) Sheldon, R. A.; Kochi, J. K. *Metal Catalyzed Oxidations of Organic Compounds*; Academic Press: New York, 1981; pp 17–32.
- (66) Bulls, A. R.; Bercaw, J. E.; Manriquez, J. M.; Thompson, M. E. *Polyhedron* **1988**, *7*, 1409–1428.
- (67) Bryndza, H. E.; Fong, L. K.; Paciello, R. A.; Tam, W.; Bercaw, J. E. *J. Am. Chem. Soc.* **1987**, *109*, 1444–1456.
- (68) (a) Thompson, M. E.; Baxter, S. M.; Bulls, A. R.; Burger, B. J.; Nolan, M. C.; Santarsiero, B. D.; Schaefer, W. P.; Bercaw, J. E. *J. Am. Chem. Soc.* **1987**, *109*, 203–219. (b) Watson, P. L. *J. Am. Chem. Soc.* **1983**, *105*, 6491–6493.
- (69) Brintzinger, H. H. *J. Organomet. Chem.* **1979**, *171*, 337–344.
- (70) Gell, K. I.; Schwartz, J. *J. Am. Chem. Soc.* **1978**, *100*, 3246–3248.
- (71) Labinger, J. A.; Bercaw, J. E. *Nature* **2002**, *417*, 507–514.
- (72) Stahl, S. S.; Labinger, J. A.; Bercaw, J. E. *Angew. Chem., Int. Ed. Engl.* **1998**, *37*, 2180–2192.
- (73) (a) Gol'dshelger, N. F.; Tyabin, M. B.; Shilov, A. E.; Shteinman, A. A. *Zh. Fiz. Khim. (Engl. Transl.)* **1969**, *43*, 1222–1223. (b) Gol'dshelger, N. F.; Es'kova, V. V.; Shilov, A. E.; Shteinman, A. A. *Zh. Fiz. Khim. (Engl. Transl.)* **1972**, *46*, 785–786.
- (74) Stahl, S. S.; Labinger, J. A.; Bercaw, J. E. *J. Am. Chem. Soc.* **1996**, *118*, 5961–5976.
- (75) Labinger, J. A.; Herring, A. M.; Lyon, D. K.; Luinstra, G. A.; Bercaw, J. E. *Organometallics* **1993**, *12*, 895–905.
- (76) Luinstra, G. A.; Labinger, J. A.; Bercaw, J. E. *J. Am. Chem. Soc.* **1993**, *115*, 3004–3005.
- (77) Luinstra, G. A.; Wang, L.; Stahl, S. S.; Labinger, J. A.; Bercaw, J. E. *J. Organomet. Chem.* **1995**, *504*, 75–91.
- (78) Zhong, H. A.; Labinger, J. A.; Bercaw, J. E. *J. Am. Chem. Soc.* **2002**, *124*, 1378–1399.
- (79) Heyduk, A. F.; Driver, T. G.; Labinger, J. A.; Bercaw, J. E. *J. Am. Chem. Soc.* **2004**, *126*, 15034–15035.
- (80) Johansson, L.; Tilset, M.; Labinger, J. A.; Bercaw, J. E. *J. Am. Chem. Soc.* **2000**, *122*, 10846–10855.
- (81) Holtcamp, M. W.; Labinger, J. A.; Bercaw, J. E. *J. Am. Chem. Soc.* **1997**, *119*, 848–849.